Environment International 162 (2022) 107162

Contents lists available at ScienceDirect

Environment International

journal homepage: www.elsevier.com/locate/envint

Full length article

Effects of African BaP emission from wildfire biomass burning on regional and global environment and human health

Min Wu [a], Jinmu Luo [b], Tao Huang [a], Lulu Lian [a], Tianlei Chen [a], Shijie Song [a], Zhanxiang Wang [a], Shuxin Ma [a], Chaoran Xie [a], Yuan Zhao [a], Xiaoxuan Mao [a], Hong Gao [a], Jianmin Ma [b,a,*]

[a] Key Laboratory for Environmental Pollution Prediction and Control, Gansu Province, College of Earth and Environmental Sciences, Lanzhou University, Lanzhou 730000, China

[b] Laboratory for Earth Surface Processes, College of Urban and Environmental Sciences, Peking University, Beijing 100871, China

ARTICLE INFO

Handling Editor: Adrian Covaci

Keywords:
Africa
Wildfire
Benzo(a)pyrene
Exposure risk
Global impact

ABSTRACT

The vegetation burning caused by wildfires can release significant quantities of aerosols and toxic chemicals into the atmosphere and result in health risk. Among these emitted pollutants, Benzo(a)pyrene (BaP), the most toxic congener of 16 parent PAHs (polycyclic aromatic hydrocarbons), has received widespread concerns because of its carcinogenicity to human health. Efforts have been made to investigate the environmental and health consequences of wildfire-induced BaP emissions in Africa. Still, uncertainties remain due to knowledge and data gaps in wildfire incidences and biomass burning emissions. Based on a newly-developed BaP emission inventory, the present study assesses quantitatively the BaP environment cycling in Africa and its effects on other continents from 2001 to 2014. The new inventory reveals the increasing contribution of BaP emission from African wildfires to the global total primarily from anthropogenic sources, accounting for 48% since the 2000 s. We identify significantly higher BaP emissions and concentrations across sub-Saharan Africa, where the annual averaged BaP concentrations were as high as 5–8 ng/m^3. The modeled BaP concentrations were implemented to estimate the lifetime cancer risk (LCR) from the inhalation exposure to BaP concentrations. The results reveal that the LCR values in many African countries exceeded the acceptable risk level at 1×10^{-6}, some of which suffer from very high exposure risk with the LCR$>1 \times 10^{-4}$. We show that the African BaP emission from wildfires contributed, to some extent, BaP contamination to Europe as well as other regions, depending on source proximity and atmospheric pathways under favorable atmospheric circulation patterns.

1. Introduction

Wildfire biomass burning, featured by forests, savannah, grassland, and other types of vegetation burning, frequently occurs across the global land areas. Wildfires play a vital role in terrestrial and climate perturbations (Bowman et al., 2009; Jolly et al., 2015; Langmann et al., 2009). It has been estimated that the global annual burned area can approach 350 Mha per year (Giglio et al., 2013). Particularly, Africa has been experiencing extensive forest, savannah, grassland, and cropland burning, accounting for 72% of burned area in the globe for the past decades (van der Werf et al., 2010). Of which, vegetation burning contributed over 90% to biomass burning, whereas the agricultural fires (crop residue burning) contributed merely about less than 10% to the total biomass burning (Kaiser et al., 2012; Lammel et al., 2013). In recent years, the frequency of extreme weather events has been increasingly associated with global warming, which is often accompanied by high temperature, drought, and low precipitation (IPCC, 2014).

Consequently, the frequency and risk of wildfire have significantly enhanced (Abatzoglou & Williams, 2016; Jolly et al., 2015). Concerns have been raised for wildfires because biomass burning provides primary sources of atmospheric aerosols and toxic chemical emissions. Of those toxic chemicals released from biomass burning, polycyclic aromatic hydrocarbons (PAHs) are produced as the byproducts of forest and vegetation fires, in addition to the incomplete combustion of fossil fuels. The widespread occurrence of PAHs has caused severe adverse effects on ecosystems and human health (Arinaitwe et al., 2012; Ke et al., 2017; Kim et al., 2013; Shen et al., 2013). Although wildfires in Africa contributed the most to the global total that caused severe air pollution

* Corresponding author at: Key Laboratory for Environmental Pollution Prediction and Control, Gansu Province, College of Earth and Environmental Sciences, Lanzhou University, Lanzhou 730000, China.

E-mail address: jmma@pku.edu.cn (J. Ma).

https://doi.org/10.1016/j.envint.2022.107162
Received 15 November 2021; Received in revised form 17 February 2022; Accepted 22 February 2022
0160-4120/© 2022 The Author(s). Published by Elsevier Ltd. This is an open access article under the CC BY license (http://creativecommons.org/licenses/by/4.0/).

and health consequences, the continental-scale assessment of African wildfire induced PAH contamination and health impact are still lacking due to the lack of in-situ measurements across the continent, particularly in sub-Saharan African countries, the places experiencing most severe wildfires in the world (Kalisa et al., 2018). The out-of-date PAH emission inventory (Zhang & Tao, 2009) that didn't sufficiently account for wildfire biomass burning emissions also caused large uncertainties in the assessment of PAH environmental contamination regionally and globally (Luo et al., 2020).

Like many persistent organic pollutants (POPs), PAHs undergo long-range atmospheric transport (Friedman & Selin, 2016; Ravindra et al., 2008; Wilcke, 2007), as evidenced by their presence in the remote, pristine Arctic environment (Friedman & Selin, 2012; Friedman et al., 2014; Yu et al., 2019; Lian et al., 2022). The health effect of PAHs has also been demonstrated in many previous studies (Ezike et al., 2017; Lammel et al., 2013; Ofori et al., 2020). Epidemiological studies have identified that long-term exposure to PAH contaminated air was often associated with an increased risk of cardiovascular disease and cancer in the general population and pregnancy outcomes (Cogliano et al., 2005; Situma, 2010; Sram et al., 2007). Embryonic toxicity and chromosomal aberrations in vivo and in vitro studies have also been reported (Le Bihanic et al., 2014; Rossner et al., 2010). Given their adverse impacts on human health and cancer diseases, such as skin cancer (Tsai et al., 2001; Wang et al., 2015) and lung cancer (Chen et al., 2008; Sarigiannis et al., 2015). In addition to carcinogen (group 1) and potential (group 2A) carcinogen, some PAHs are also classified as possible carcinogen (group 2B) by the International Agency for Research on Cancer (IARC, 2021; Situma, 2010; Zhang et al., 2021), the United States Environmental Protection Agency (Bortey-Sam, 2011; EPA, 1993). Typically, Benzo(a)pyrene (BaP) as the most toxic congener of parent PAHs was often used as an indicator of PAHs (Situma, 2010). Given its mutagenic and highly carcinogenic effects through several exposure routes (Agudelo-Castaneda et al., 2017; Rengarajan et al., 2015; Zhang et al., 2021), BaP has been classified into Group 1 carcinogen by the IARC (IARC, 2021; Shen et al., 2014). BaP has been widely detected in multiple environments worldwide, though not manufactured and used in industry. The presence of BaP in the environment is often attributed to its formation during the combustion of organic matter (Ofori et al., 2020) and its emissions from natural sources in forest fires and volcanic eruptions (Menzie et al., 2002; Zedeck, 1980). The anthropogenic emissions of BaP can be sourced from the combustion of fossil fuels and motor vehicles (Ravindra et al., 2008; Wilcke, 2007).

The present study sets out to assess the PAH contamination and cycling quantitatively in Africa using a modified global atmospheric transport model coupled with multi-compartment exchange modules and corresponding health consequences. The model framework used in this study allows us to take advantage of the high temporal-spatial resolution of BaP distribution and source-receptor relationships across Africa and assess global PAH contamination sourced from Africa. The results could help PAH emission reduction and mitigation and reduce exposure risks in the African population. A new global emission inventory of PAHs from biomass burning also provides a unique dataset in this numerical investigation. This new inventory used recent global forest carbon stocks and considered all small and moderate fires (Giglio et al., 2009; Luo et al., 2020), many of which were missing in previous inventories and PAH modeling, leading to the over-or under-estimation of PAH contaminations in some eco-sensitive environments by up to a factor of 2–3 (Lammel et al., 2013).

Using the updated BaP emission inventory, the present study simulated the global BaP cycling from 2001 to 2014, focusing on Africa. The objectives of the present study are to (1) paint an overall picture of wildfire induced BaP contamination in Africa, (2) fill knowledge gaps in the understanding of the contribution of African wildfire biomass burning to its environment and health consequences on a high temporal-spatial resolution, (3) identify the significant sources from wildfires and their impacts on surrounding sub-Saharan African countries, and (4) assess the impact of African PAH emissions from wildfires on the global environment. The study aims to provide scientific support to the environment and health management, and emission mitigations.

2. Data and methodology

2.1. Emission inventory

An updated BaP global wildfire biomass burning emission inventory (Luo et al., 2020) was adopted in the present study, which extended from 2001 to 2014 based on the availability of the global carbon stock inventory. The inventory was developed based on global carbon stocks and improved emission factors by combining widely-used bottom-up forest carbon stock inventories from Pan et al. (2011) and the Global Forest Resources Assessment (GFRA, https://www.fao.org/forest-resources-assessment/en/). It is worth noting that the GFRA just recently updated the global carbon stock inventory to 2020. The updating of our PAH emission inventory from wildfire biomass burning after 2014 is also underway. To better present the global vegetation biomass carbon stocks, the inventory took savanna, grassland, prairie, and the herb carbon stocks into account, derived from MODIS satellite dataset MOD17A3H and burned area Collection 6 dataset (MCD64CMQ dataset). The inventory includes most types of vegetation biomass burning and surface biomass distribution on a $1^\circ \times 1^\circ$ latitude/longitude resolution. This inventory has been employed to assess the PAH contamination and source tagging across the Arctic using the global-scale Geos-Chem atmospheric chemistry model (Luo et al., 2020). The results showed significant improvement in BaP prediction across the Arctic. The present modeling investigation study will focus on BaP as the target PAH congener due to its highest cancer risk among the 16 parent PAHs listed by the USEPA. Its global emission inventory was extracted from the updated PAH wildfire biomass burning inventories (Luo et al., 2020).

2.2. CanMETOP

The Canadian Model for Environmental Transport of Organochlorine Pesticides (CanMETOP, Ma et al.(2003)) was employed in the study. The CanMETOP is a three-dimensional atmospheric transport model for POPs coupled with POPs' multi-compartment exchange modules. The model has a horizontal resolution at $1^\circ \times 1^\circ$ (latitude/longitude) covering the globe and 14 vertical levels from 0, 1.5, 3.9, 10, 100, 350, 700, 1200, 2000, 3000, 5000, 7000, 9000, to 11000 m, respectively. The CanMETOP was developed based on the atmospheric advection/diffusion equation with a terrain-following coordinate, combined with the air-to-soil exchange module based on the IV-level fugacity method and air-to-water exchange module based on the two-thin film theory. The model is solved numerically by a finite-difference approximation and operator-splitting scheme. The advanced boundary layer parameterization scheme featured by a non-local turbulence closure is employed to predict the cycling of organic chemicals within the atmospheric boundary layer. The meteorological data driving CanMETOP, including winds, atmospheric pressure, temperature, and precipitation rate, were collected from 6-hourly (00, 06, 12, 18 UTC) objective reanalysis data from National Centers for Environmental Prediction (NCEP) Final Operational Global Analysis dataset (https://rda.ucar.edu/datasets/ds083.2/). This dataset has a spatial resolution of $1^\circ \times 1^\circ$ lat/long, the same as the CanMETOP grid spacing. The 6-hourly met data were interpolated into the CanMETOP time step length at 20 min. More details about the CanMETOP are referred to Ma et al. (2003) and Huang et al. (2020).

2.3. Model setup, validation, and uncertainty

The CanMETOP model was integrated from 2001 to 2014, with the first three months (January 1st to March 31st, 2001) as the spin-up

period. To assess the relative contribution of the BaP emissions from PKU-FUEL and the present study, we set up two model scenarios using BaP emission inventory from the wildfire biomass burning and PKU-FUEL BaP inventory from all sectors, referred to as model scenarios S1 and S2, respectively. In addition, another two model scenario simulations (S3, S4) are carried out for 2010 to explore the contribution of African BaP emissions from wildfire biomass burning to its contamination in other countries and regions outside Africa. The details are presented in **SI Text 1**. We employed a first-order error propagation approach to examine the model uncertainties (Huang et al., 2020; MacLeod et al., 2002). We identified that primary uncertainties were attributed to emissions, physicochemical properties, and some atmospheric removal processes, such as dry deposition. We estimated an overall uncertainty of the modeled BaP concentration from wildfire burning with a factor of 1.02 to 3.99. Details are presented in **SI Text 2**.

The modeling results were validated against measurement data in Africa and Europe. Due to scarce ambient BaP sampling data across the African continent, the model validation in Africa was only conducted by comparison with limited sampling data during the modeling investigation period. Supporting Information (SI) **Table S1** and **Figs. S1 and S2** presents field campaigns for PAH sampling conducted in several African countries and the comparisons between modeled BaP concentrations using the wildfire emission inventory (model scenario S1) and PKU-FUEL BaP emission inventory (model scenario S2) and sampled data. **Fig. S3** presents a correlation diagram between modeled BaP air concentrations derived from PKU-FUEL BaP emission inventory and sampled data across Europe collected from 2001 to 2014. Details are presented in **SI Text 3**.

2.4. Lifetime cancer risk assessment

We used a widely applied methodology proposed by the USEPA to evaluate the lifetime lung cancer risk in Africa due to inhalation exposure to BaP subject to wildfire burning, derived using BaP equivalent concentration (BaPeq). As mentioned above, due to its high carcinogenic risk, BaP was taken as the indicator of PAHs carcinogenic risk in this study, which has been extensively investigated in previous studies (Abdallah & Atia, 2014; Callen et al., 2014; Feng et al., 2019; Hoseini et al., 2016; Kalisa et al., 2018; Zheng et al., 2018). The carcinogenic risk is often associated with the toxicity equivalence factor (TEF) of each PAH compared to BaP (Kalisa et al., 2018). BaPeq is calculated by multiplying the concentration of each PAH with its corresponding TEF. Since the focus of the present study was on BaP, we only took BaPeq of BaP with its TEQ as a unity (Collins et al., 1998) into consideration. The lifetime cancer risk (LCR) from the inhalation exposure to BaP can be estimated as follows:

$$LCR = URBaP \times BaPeq \quad (1)$$

where URBaP is the inhalation cancer unit risk factor of BaP, and URBaP is defined as the number of people who have a higher cancer risk due to inhalation exposure to an equivalent BaP concentration of 1 ng/m^3 spanning a lifetime of 70 years (Callen et al., 2014; Orakij et al., 2017). According to the Office of Environmental Health Hazards Assessment (OEHHA) of the California Environmental Protection Agency (CalEPA), URBaP can be taken as 1.1×10^{-6} (ng/m^3)$^{-1}$. The WHO (World Health Organization) suggested URBaP value at 8.7×10^{-5} (ng/m^3)$^{-1}$. This study used both URBaP values to assess the health risk due to human exposure to BaP.

3. Results and discussion

3.1. BaP emission from wildfire biomass burning

Fig. 1 shows mean BaP emissions from forest and vegetation fires across the globe, averaged from 2001 to 2014. Gridded annual emissions during the same period are shown in **Fig. S4**. Higher emissions can be discerned in sub-Saharan Africa, followed by North Africa, Brazil, and Southeast Asia. In some sub-Saharan countries in southern and central Africa, emissions reach as high as 1000–8000 kg per year.

Fig. 2 shows changes in annual BaP emissions (10^6 kg) from all sectors averaged over the globe from PKU-FUEL (solid deep blue line) and wildfire biomass burning over the world (solid deep red line) and Africa (solid green line), developed in this study. The solid grey line, scaled on the right Y-axis, represents the ratio of BaP emissions from African wildfire burning from this study to the emission from all sectors in PKU-FUEL inventory. The results indicate no significant differences between global and African BaP emissions from wildfire burning. They suggest that African wildfire biomass burning contributed the majority of BaP emission to its global total, in line with previous investigations (Lammel et al., 2013; Lian et al., 2021; Luo et al., 2020; Shen et al., 2013). The wildfire biomass burning induced mean emission in Africa averaged over 2001 to 2014 accounted for 82% of its global total. After reaching their respective peak values in 2003 and 2005, we noticed that BaP emissions from all sectors (PKU-FUEL) and wildfire burning in the globe and Africa (this study) declined. Considering that wildfires induced-BaP emissions in Africa dominated its global emission from wildfire burning, it is not surprising to observe similar annual

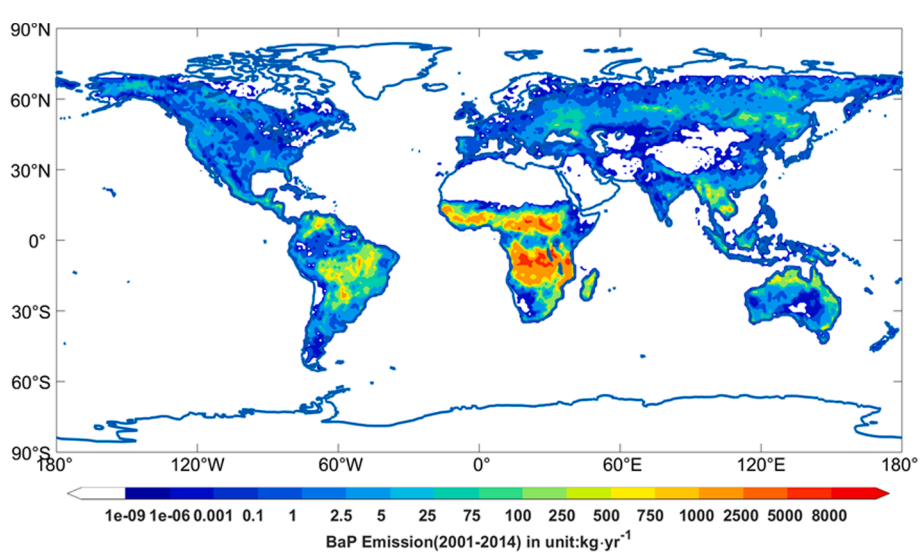

Fig. 1. Mean BaP annual emissions (kg/year) from wildfire biomass burning averaged from 2001 to 2014.

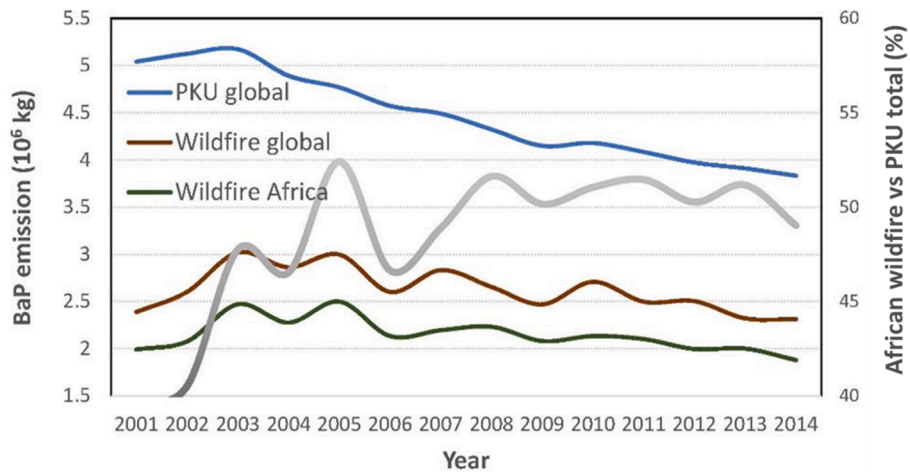

Fig. 2. Annual variations of global total BaP emissions (10^6 kg/year) from all sectors in PKU-FUEL (solid blue line), wildfire biomass burning over the globe (solid deep red line), and Africa (solid green line) from 2001 to 2014 developed in this study. These emissions are scaled on the left Y-axis. The thick grey line represents mean emission ratios (%, scaled on the right Y-axis) of African wildfire biomass burning (this study) to PKU-FUEL total BaP emission.

fluctuations in wildfire emissions in Africa and global BaP emissions. This can also be seen from the variation of annual burned area in Africa from 2001 to 2014 (**Fig. S5,** yellow shading), which shows the larger burned area from 2003 to 2005 compared to the rest of the years.

A previous study (Lammel et al., 2013) has reported the global and African BaP emissions from biomass burning at 1.4×10^6 kg and 7.2×10^5 kg in 2008, respectively, indicating that African BaP emissions contributed 53% to the global total from biomass burning. Our estimated wildfire biomass burning induced annual emission is 20.2×10^5 kg, almost a factor of three higher than Lammel et al.'s result. We found that the mean emission averaged over 2001 to 2014 in Africa contributed 82% to the total global emission from wildfires. It has been projected that African combustion emission would account for 50% of the global total due to the growing emission in Africa and declining emission in the rest of the world (Liousse et al., 2014). Our results reveal increasing ratios of African BaP emissions from the wildfire burning to BaP emissions from all sectors in the globe with a mean ratio of 0.48. The result indicates that the wildfire burning emitted BaP in Africa alone contributes almost 50% to its global total from all sectors! Given continuously decreasing BaP emissions from anthropogenic sources due to worldwide emission control, it is likely that African emissions from wildfire biomass burning could dominate global PAH emission and contamination (Fig. 2). It has been reported that the BaP emissions from biomass burning in the PKU-FUEL inventory were underestimated markedly, especially for Africa and the Arctic (Luo et al., 2020), and likely resulted from emission factors and burned area data in the construction of PKU-FUEL inventory and this study. The new wildfire emission adopted an updated MODIS burning area dataset, which considered sufficiently small fires and improved emission factors (Luo et al., 2020). Whereas, such small fires and burned areas were not considered in previous inventories due to the lack of data.

3.2. Modeled BaP concentration in air

Fig. 3**a and 3b** show modeled mean BaP air concentrations in gas (Fig. 3**a**) and particle (Fig. 3**b**) phase, averaged over Africa from 2001 to 2014. As expected, a similar spatial distribution pattern can be discerned in simulated gas and particle-phase concentrations, in line with its emissions with significantly higher particle-phase concentrations, as demonstrated previously (Hassan & Khoder, 2012; Ramirez et al., 2011; Verma et al., 2017). From a global perspective, we found that the mean gas to particle BaP concentration ratio averaged over 2001 to 2014 was 0.23 using all sector PKU-FUEL inventory and 0.08 using the updated BaP inventory from the wildfire burning in this study, respectively. The result seems to suggest that BaP concentrations emitted from wildfire biomass burning tend to be more strongly partitioned into particle-phase. It is not clear yet the wildfire emission-induced stronger BaP partitioning into the particle phase, but likely the open biomass burning could yield higher particle-bound BaP concentrations than non-open burning emissions (Chiu et al., 2011). For Africa, the both model S1

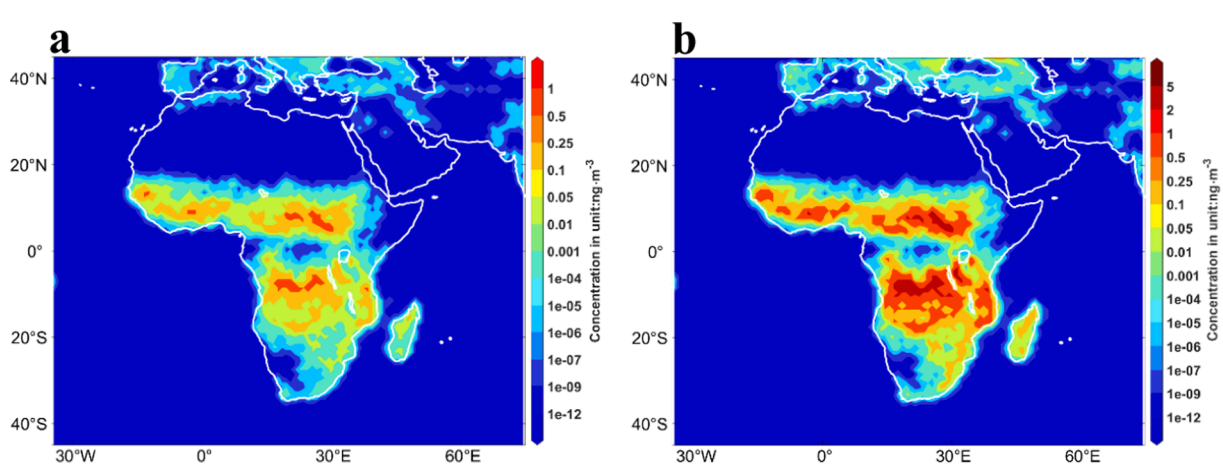

Fig. 3. Mean gas (a) and particle (b) phase BaP atmospheric concentration (ng/m^3) over Africa averaged from 2001 to 2014.

and S2 simulations yielded similar ratio at about 0.24, which is almost identical to the wildfire burning-induced global BaP gas-particle ratio. Because in PKU-FUEL inventory the BaP emissions in Africa were also dominated by wildfire burning, we could expect a similar gas-particle ratio to that from updated BaP inventory from the wildfire burning. It is worthwhile to note that annual mean total (particle + gas) BaP concentration near the surface (the first model level at the 1.5 m height above the ground surface) was well above 1 ng/m^3 in many areas of sub-Saharan Africa (**Fig. S6**). This value was considered as a threshold value (1 ng/m^3) for human health risk recommended by the European Environment Agency in 2011 (EEA, 2019) and far above the WHO (World Health Organization, 2017) reference level of 0.12 ng/m^3 for life-time cancer risk at 10^{-5}. **Fig. S6** in SI shows the simulated annual BaP atmospheric concentrations from wildfire biomass burning over Africa from 2001 to 2014, illustrating a similar spatial pattern to the emission sources in forest and savannah covered areas (**Fig. S5**).

In line with the updated wildfire emissions, higher BaP atmospheric concentrations are mainly identified in sub-Saharan Africa, the areas extending from north to south Congo Basin, which agrees with previous modeling results of Lammel et al. (2013). The mean BaP concentration averaged over the continent from 2001 to 2014 was 0.18 ng/m^3, which is almost one order of magnitude higher than Lammel et al.'s result at 0.02 ng/m^3 averaged over January–June 2008. As shown in Fig. 3, the mean concentrations in some sub- Saharan African regions were as high as 5–8 ng/m^3 with the maximum reaching 10 ng/m^3, again greater than those simulated BaP concentrations by Lammel et al. (2013) in the same regions, which is mainly attributed to higher BaP emissions from the wildfire burning developed in this study.

Like emissions, the modeled BaP concentrations using the PKU-FUEL all sector emissions illustrate a downward trend in the globe (slope = -3.5 × 10^{-3}, R^2 = 0.88 Fig. 4**a**) and Africa (slope = -7 × 10^{-4}, R^2 = 0.36, Fig. 4**b**) from 2001 to 2014, though fluctuated in Africa (Fig. 4**b**). Such declining trends are also observed in BaP fluctuations using the wildfire emission inventory (solid deep red lines). In Africa, simulated BaP concentrations from wildfires in the present study are factors of 2 higher than those emitted from PKU-FUEL anthropogenic sources. This could, again, be attributed to significant underestimation of BaP emissions from the wildfire biomass burning due to ignoring small burned areas in the previous emission inventories (Lammel et al., 2013; Shen et al., 2013). Previous study (van der Werf et al., 2010) has reported that Africa contributed the most to the global total burned areas, accounting for 72% from 1997 to 2009 with an annual rate of increase 2.3 Mha yr^{-1} during this period but declined since 2000 at an annual rate of 1.7 Mha yr^{-1} in Southern and Northern Hemispheric Africa, respectively (Giglio et al., 2013). Our data revealed the total burned area of 3.94 × 10^3 Mha and active fires of 1.736 × 10^7 MW in Africa summed from 2001 to 2014, accounting for 66% and 34% of their respective global total. As mentioned before, emission underestimations were particularly evident in Africa, where BaP emissions were overwhelmed by wildfire biomass burning. The dominant BaP emission and concentration in Africa could

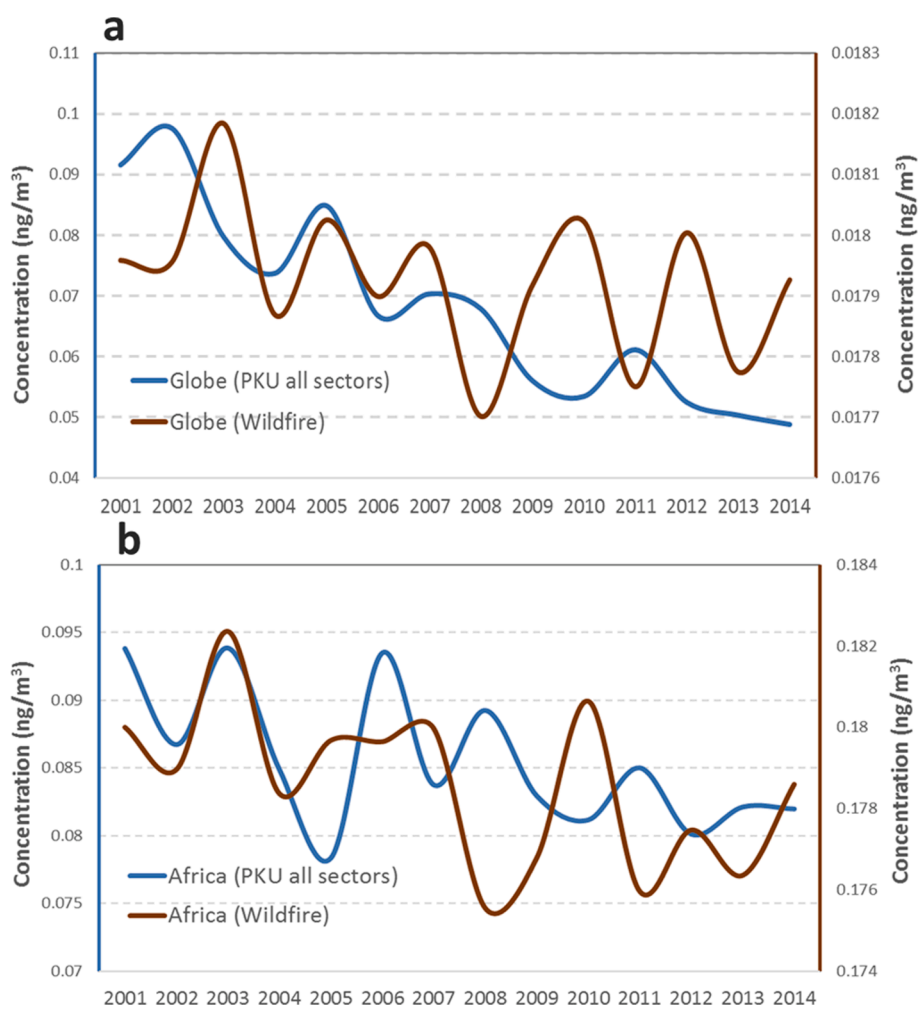

Fig. 4. Modeled mean annual BaP air concentrations (ng/m^3) from 2001 to 2014 averaged over all model grid cells across the model domain (Fig. 4**a**) and Africa (Fig. 4**b**) using the PKU-FUEL BaP inventory from all source sectors (solid blue line, scaled on the left Y-axis) and emissions from wildfire biomass burning (solid red line, scaled on the right Y-axis).

also be associated with the burned area and meteorological conditions, such as precipitation and air temperature. Fig. S7 shows changes in modeled annual BaP concentration, emissions from wildfire biomass burning (E), burned areas (BA), and the anomalies of mean air temperature at the 2 m height (K) and precipitation water (kg/m^2), averaged over sub-Saharan Africa (30°S–10°N, 10°–50°E). The temperature and precipitation water anomalies are estimated as the departure from their respective means from 1981 to 2010. As seen, modeled BaP concentration fluctuations in Africa responded positively to the burned area and emission from wildfires, but inversely to the precipitation water anomalies, featured by increasing concentrations with decreasing precipitation water anomalies. The latter indicates a good association between wildfire emissions and drought climate characterized by low precipitation water. However, the variation of annual concentrations seems not associated well with the mean air temperature.

Given that coal combustion-related sources contribute primarily to PAH emissions (Shen et al., 2013), we observe that the global mean BaP concentrations driven by PKU-FUEL all source emissions are about a factor of 4 higher than that from biomass burning. It is worth noting that, although the summed BaP emission from wildfire biomass burning over the globe (Luo et al., 2020) contributed 48% to the total global emission from all sectors (Shen et al., 2013), as mentioned above, the global mean BaP concentration averaged over all model grid cells in the global model domain from 2001 to 2014 merely accounts for 27% of mean BaP concentration predicted by CanMETOP using PKU-FUEL emissions from all sectors. This is because most summed emissions from wildfires occurred in Africa (Figs. 1 **and S1**); strong BaP emission from African wildfire results in its increasing share in the total global emission from all sectors. On the other hand, the mean concentration is reduced significantly by grid cells where concentrations are very low or nil after taking the global average. Figs. S8 and S9 illustrate modeled annual BaP concentrations using the emissions from wildfire biomass burning (model scenario S1) and the PKU-FUEL BaP emissions from all sectors (model scenario S2). Higher concentrations from the S2 scenario simulation can be observed in China and India, consistent with BaP anthropogenic emissions. In contrast, the S1 model scenario yields a higher concentration in Africa. Both inventories produce the maximum concentrations at almost the same order of magnitude.

3.3. Effect of African wildfire emission on global BaP pollution

Considering the significant contribution of African wildfire emission to the biomass burning sector and all sources in Africa and the globe, we estimated the fraction of African wildfire-induced BaP concentration to other continents and countries (**SI Text 1**). Fig. 5 displays the fractional contribution of African wildfire emitted BaP to its levels in different continents in four seasons of 2010. These contributions depend on the proximity of receptor regions to the African sources and changes in atmospheric circulations and prevailing wind systems. Our results identify that the autumn season favors mostly the long-range transport of BaP from Africa to other continents, followed by winter, summer, and spring, respectively. We also show that, in all seasons, the largest contribution of African biomass burning to BaP contamination in different receptors outside Africa occurred in Southern Europe, followed by South America, Western and Northern Europe, Antarctic, the United States (US) (mostly the Southeastern US), and the Arctic. Previous studies reported that African dust could transport across the Atlantic Ocean to South America (Prospero et al., 1981), the US (Carder et al., 1986; Prospero & Carlson, 1972; Savoie & Prospero, 1977), and Europe (Ansmann et al., 2003; Mattsson & Nihlén, 1996; Perry et al., 1997; Stuut et al., 2009). Such

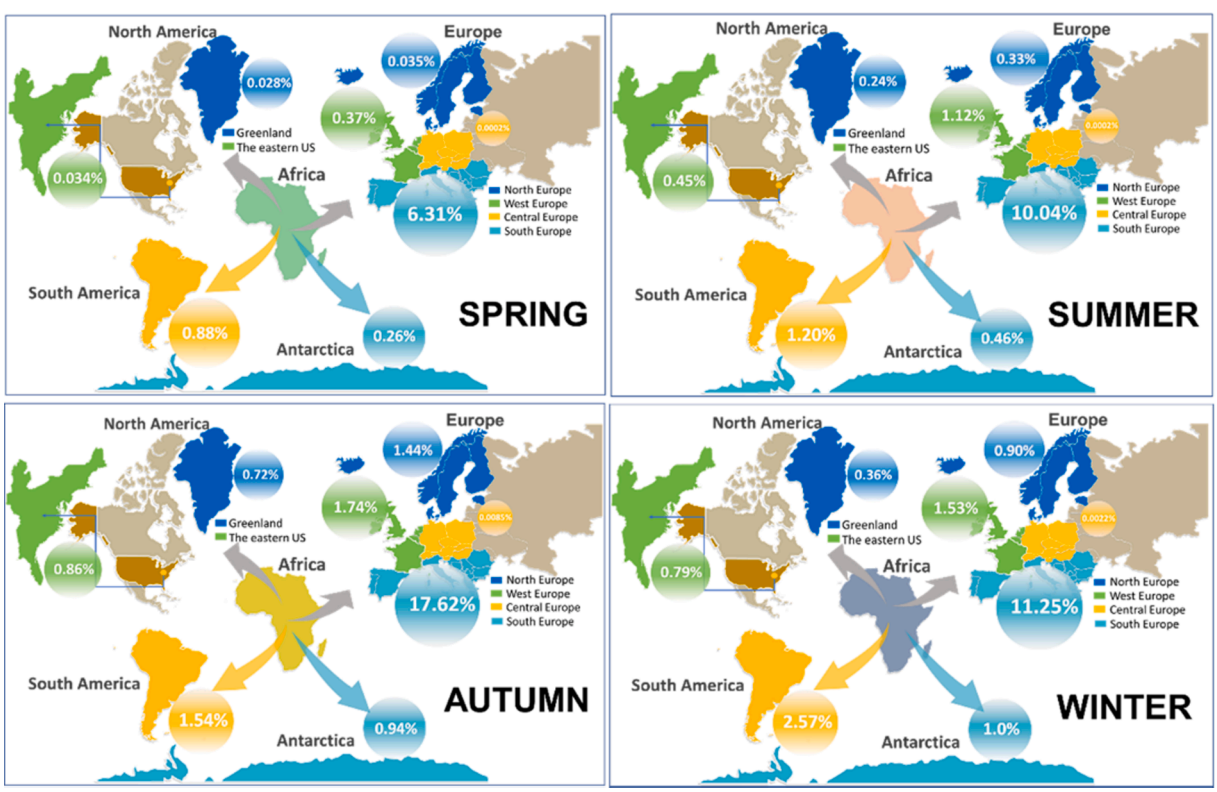

Fig. 5. Percentage contribution $(C_{s3} - C_{s4}) \times 100/C_{s4}$ of modeled BaP concentrations from African wildfire biomass burning to different regions in different seasons of 2010, where C_{s3} and C_{s4} (ng/m^3) are the simulated BaP concentration at 850-hPa (~1500 m) from the model scenarios S3 and S4 (**SI Text 1**) in 2010, respectively. The arrows indicate the export of BaP concentrations from Africa to targeted regions. The sizes of pies are proportional to the contribution of African wildfire biomass burning induced BaP concentrations to the other areas. The percentage in each pie indicates the contribution fractions, defined as the proportion of the BaP concentration difference from two modeling experiments (S3 and S4) to that of the second experiment (S4) with African emissions closed, which can be referred to **SI** eq **S1**.

dust transport is mainly due to the northward shift of the intertropical convergence zone (ITCZ), the easterly trade wind, low-level African easterly jet (AEJ), and prevailing wind systems. Among these transport pathways, the low-level southerly winds (Prodi & Fea, 1979) provide a transport route of African dust to Southern Europe, even approaching Western and Northern Europe (Barkan, 2005). A close look at the wind patterns for the four seasons at 850-hPa (about 1500 m height above the ground surface, **Fig. S10**), one could discern stronger southerly and southwesterly flows along the west coast of Northern Africa extending southern Europe, particularly in autumn. These wind systems accompany weak Azores High across the North Atlantic Ocean. This route also delivers BaP emitted from African wildfires to Europe, accounting for 17.6%, 11.3%, and 10% of total BaP levels in Southern Europe in autumn, winter, and summer, respectively (Fig. 5). The easterly trade wind system has been reported to drive westward transport of Saharan dust and air pollutants from Africa to the US and Southern America. We can also identify strong seasonally averaged easterly trade winds along the Equator, particularly in the wintertime. This robust winter easterly wind system in the south of the Equator drove more BaP concentrations from Africa to South America (**Fig. S10**). Zhang et al. (2008) have identified the episodic *trans*-Atlantic transport of lindane from western Africa to North America and attributed such transport to the well-known easterly trade wind and the west extension of African easterly wave.

Since we only present seasonal mean wind systems (**Fig. S10**), we did not observe significant seasonal contribution (less than 1%) of African wildfire emitted BaP on the US, likely the presence of combustion-induced relatively high BaP levels in the US. Less significant BaP transport from Africa occurs in the Arctic due to the pristine polar region to Africa. In addition, since the major PAH emissions from wildfire biomass burning occurred in sub-Saharan Africa in the Southern

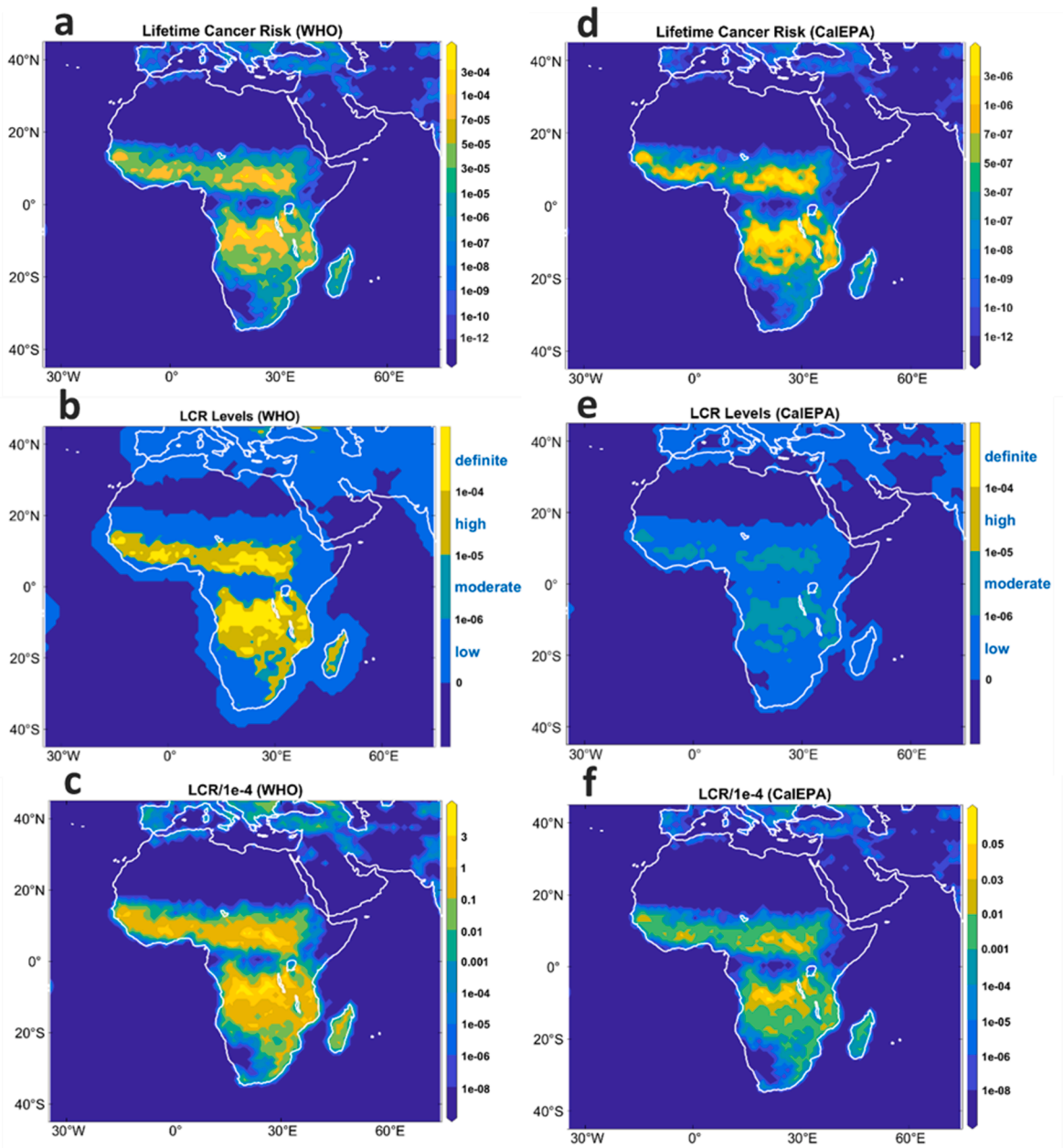

Fig. 6. Lifetime cancer risk (LCR) from inhalation exposure to BaP emitted wildfire biomass burning. (a) LCR estimated based on WHO approach (URBaP = 8.7×10^{-5}); (b) LCR distribution associated with four risk levels, defined as definite ($>1 \times 10^{-4}$), high (1×10^{-5}–1×10^{-4}), moderate (1×10^{-6}–1×10^{-5}), and low (less than 1×10^{-6}) risks subject to the WHO defined URBaP; (c) ratio of estimated LCR to the threshold LCR of 1×10^{-4} subject to WHO defined URBaP. (d-f) same as Fig. 6**a-c** but for LCR based on CalEPA defined URBaP ($=1.1 \times 10^{-6}$).

Hemisphere, the weak cross-equator wind flow is not an efficient pathway for the cross-equator transport of air pollutants to the US, as compared to the transport route to South America where the 2.6% of BaP concentration came from Africa. This can also be demonstrated by the higher percentage contribution of the atmospheric transport from Africa to the Antarctic than the Arctic.

3.4. Health risk assessment

Based on the simulated BaP atmospheric concentration from wildfire burning, we assessed the health consequences of biomass burning-induced BaP contamination by estimating the LCR in Africa with two threshold values recommended by the WHO (URBaP = 8.7×10^{-5} (ng/m^3)$^{-1}$) and the CalEPA (URBaP = 1.1×10^{-6} (ng/m^3)$^{-1}$). Fig. 6 shows the estimated LCR in Africa based on these two threshold values. As expected, the WHO-recommended URBaP value (Fig. 6**a**) yields higher inhalation exposure risks in African residents than from the CalEPA, with the maximum LCR reaching 0.0007, indicating 70 cancer cases per 100,000 population. The latter predicts the maximum 1 LCR cases per 100,000 population (Fig. 6**d**) but illustrates identical spatial distribution across Africa from the WHO approach. Higher LCR values can be observed in Sub-Saharan Africa, especially those countries around Congo Basin.

We further highlight the regions across Africa where the LCR exceeds the acceptable risk threshold values based on the URBaP provided by the WHO and CalEPA. Following previous studies, we selected four risk levels according to the USEPA and WHO guidelines and other studies (Hoseini et al., 2016; Sexton et al., 2007; Zheng et al., 2018). We refer to the threshold LCR value of 1×10^{-4} as the "definite risk," 1×10^{-5} as "high risk" (WHO guideline, (Feng et al., 2019; Orakij et al., 2017)), 1×10^{-6} as the "moderate risk" (Callen et al., 2014; Kalisa et al., 2018), which is an acceptable risk level in the USEPA guideline (Kalisa et al., 2018; Ramirez et al., 2011), and below 1×10^{-6} as the "low risk" (Sexton et al., 2007). The results of these risk levels are displayed in Fig. 6**b and 6e.**

As seen, some regions in and around Congo Basin and the seaboard of southern coast of West Africa are within the "definite risk" with the LCR level $\geq 1 \times 10^{-4}$ regime under the WHO standard. The high risk regions ($10^{-5} <$ LCR $\leq 10^{-4}$) superimposed with the "definite risk" region but expanded to much large areas. The regions under the "low risk" are primarily distinguished in the southern edge of Saharan Africa, most of Namibia, and the coastal areas of Africa. Under the CalEPA standard, the definite and high-risk areas are not identified but moderate risk areas cover the same areas as those regions with definite and high risk subject to the WHO standard (Fig. 6**b**), mainly in northeast Angola, southwest South Sudan, the south of the Democratic Republic of the Congo. The results suggest that those countries and regions around Congo Basin and western Africa become high and moderate risk areas. Under the CalEPA standard, the LCR in Africa was still within low to moderate risk regime (Fig. 6**e**). Overall, the LCR in most sub-Saharan Africa exceeds the acceptable risk criteria of 1×10^{-6} subject to both WHO and CalEPA, notably the areas in and around the Congo Basin. This can be further demonstrated by a risk ratio (Fig. 6**c and 6f**), calculated as LCR divided by "definite risk" level, namely, LCR/(1×10^{-4}). Those areas with a risk ratio > 1 are regarded as the high-risk regions. As shown in Fig. 6**c,** most sub-Saharan African countries exceed the risk ratio of 1 under the WHO guideline. In the south of the Congo Basin and southwestern South Sudan, the LCR reaches three times the risk ratio. Low-risk regions are found, for example, in Madagascar, where the ratio ranges from 0.01 to 0.1. However, we did not identify any high-risk regions across Africa according to the CalEPA guideline.

4. Conclusions

Africa contributed more than half of biomass burning globally, which releases a massive amount of harmful air pollutants, including PAHs. The present study updated global BaP emissions from wildfire biomass burning using recently released forest and vegetation carbon stock inventories from 2001 to 2014. Extensive model simulations were carried out to quantify environmental contamination, human exposure risks, and source-receptor relationships for BaP with a focus on Africa. Our modeled BaP levels in Africa were as high as 5–8 ng/m^3 and even reached 10 ng/m^3 in some areas. While we found that annual mean BaP concentrations averaged over the globe using PKU-FUEL total sector emissions were almost a factor of 4 higher than that from the wildfire biomass burning, the annually averaged concentration induced by the wildfire burning in Africa was nearly a factor of 2 higher than that simulated using PKU-FUEL BaP emission from total sectors. We showed that, along with worldwide decreasing BaP emissions from anthropogenic sources in the past decade, the contribution of African wildfire emissions to the global total enhanced and tended to overwhelm, likely foreseeing an anthropogenic to nature emission transition. We identified that as high as 17% of BaP concentrations in southern Europe could be traced back to Africa. The wildfire biomass burning in this continent also contributed, to different extents, to South America, as well as Western and Northern Europe, attributable to source proximity and favorite atmospheric circulations. Significantly higher inhalation exposure risks were modeled in Africa, particularly in sub-Saharan African countries, such as those around Congo Basin. Our results indicated that the lifetime cancer risk (LCR) subject to the WHO and CalEPA guidelines in sub-Saharan African countries exceeded the acceptable risk criteria (the bottom risk line) of 1×10^{-6}. Under the WHO standard, the LCR in these countries and regions of African continent exceeded the high-risk threshold of 1×10^{-4}, causing considerably high human exposure risk in African residents.

Along with the continuous reduction of PAH emissions from fossil fuel combustion under global mitigation of carbon dioxide and air pollutant emissions, it is expected that wildfire biomass burning would play an increasingly important role in PAH contaminations and health risks worldwide. Actions should be taken in Africa, the largest source of PAH released from wildfires globally, to reduce wildfire biomass burning emission in the continent. More studies need to be carried out to enhance our understanding of primary sources, the influences of environmental conditions and human activities on wildfire emissions, and the health responses of African residents to PAH pollution induced by wildfire burning. In light of this, extensive field campaigns need to be conducted across Africa during wildfire burning and non-burning periods. More samples of cancer diseases in African countries need to be collected. The data could help more precisely assess the associations between African wildfire biomass burning and PAH contamination and health consequences. The Task Force on Hemispheric Transport of Air Pollution (HTAP) under the auspices of the UNECE (the United Nations Economic Commission for Europe) Convention on Long-range Transboundary Air Pollution (LRTAP Convention) has recently updated the burnt-related PAH/BaP emission, modeling, and model intercomparison program (http://htap.org/events/). The launch of this program suggests an increasing concern from international communities on PAH emission from wildfire burning and health impact, which could inspire more PAH-related investigations in Africa.

CRediT authorship contribution statement

Min Wu: Methodology, Visualization, Formal analysis, Writing - original draft, Writing – review & editing. **Jinmu Luo:** Data curation, Investigation, Writing-review & editing. **Tao Huang:** Supervision, Software, Formal analysis. **Lulu Lian:** Investigation, Software, Formal analysis. **Tianlei Chen:** Methodology, Formal analysis. **Shijie Song:** Validation, Investigation. **Zhanxiang Wang:** Formal analysis, Validation. **Shuxin Ma:** Investigation, Formal analysis. **Chaoran Xie:** Investigation. **Yuan Zhao:** Software. **Xiaoxuan Mao:** Formal analysis. **Hong Gao:** Project administration, Resources. **Jianmin Ma:** Conceptualization, Supervision, Writing – review & editing.

Declaration of Competing Interest

The authors declare that they have no known competing financial interests or personal relationships that could have appeared to influence the work reported in this paper.

Acknowledgements

This study is supported by the National Natural Science Foundation of China (grants U1806207, 41977357, and 42177351). We thank Prof. Shu Tao for providing PKU-FUEL BaP emission data.

Appendix A. Supplementary material

Supplementary data to this article can be found online at https://doi.org/10.1016/j.envint.2022.107162.

References

Abatzoglou, J.T., Williams, A.P., 2016. Impact of anthropogenic climate change on wildfire across western US forests. Proc. Natl. Acad. Sci. USA 113 (42), 11770–11775. https://doi.org/10.1073/pnas.1607171113.

Abdallah, M.-A.-E., Atia, N.N., 2014. Atmospheric concentrations, gaseous-particulate distribution, and carcinogenic potential of polycyclic aromatic hydrocarbons in Assiut, Egypt. Environ. Sci. Pollut. Res. Int. 21 (13), 8059–8069. https://doi.org/10.1007/s11356-014-2746-6.

Agudelo-Castaneda, D.M., Teixeira, E.C., Schneider, I.L., Lara, S.R., Silva, L.F.O., 2017. Exposure to polycyclic aromatic hydrocarbons in atmospheric PM1.0 of urban environments: Carcinogenic and mutagenic respiratory health risk by age groups. Environ. Pollut. 224, 158–170. https://doi.org/10.1016/j.envpol.2017.01.075.

Ansmann, A., Bösenberg, J., Chaikovsky, A., Comerón, A., Eckhardt, S., Eixmann, R., Freudenthaler, V., Ginoux, P., Komguem, L., Linné, H., Márquez, M.Á.L., Matthias, V., Mattis, I., Mitev, V., Müller, D., Music, S., Nickovic, S., Pelon, J., Sauvage, L., Sobolewsky, P., Srivastava, M.K., Stohl, A., Torres, O., Vaughan, G., Wandinger, U., Wiegner, M., 2003. Long-range transport of Saharan dust to northern Europe: The 11–16 October 2001 outbreak observed with EARLINET. J. Geophys. Res.-Atmosph. 108 (D24) https://doi.org/10.1029/2003JD003757.

Arinaitwe, K., Kiremire, B.T., Muir, D.C., Fellin, P., Li, H., Teixeira, C., Mubiru, D.N., 2012. Atmospheric concentrations of polycyclic aromatic hydrocarbons in the watershed of Lake Victoria, East Africa. Environ. Sci. Technol. 46 (21), 11524–11531. https://doi.org/10.1021/es302238w.

Barkan, J., 2005. Synoptics of dust transportation days from Africa toward Italy and central Europe. J. Geophys. Res. 110 (D7) https://doi.org/10.1029/2004jd005222.

Bortey-Sam, N., 2011. Distribution of Polycyclic Aromatic Hydrocarbons in Air and Surface Soil: Case Study Kumasi, Ghana (Master). Kwame Nkrumah University of Science and Technology. http://hdl.handle.net/123456789/4107.

Bowman, D.M.J.S., Balch, J.K., Artaxo, P., Bond, W.J., Carlson, J.M., Cochrane, M.A., D'Antonio, C.M., DeFries, R.S., Doyle, J.C., Harrison, S.P., Johnston, F.H., Keeley, J. E., Krawchuk, M.A., Kull, C.A., Marston, J.B., Moritz, M.A., Prentice, I.C., Roos, C.I., Scott, A.C., Swetnam, T.W., van der Werf, G.R., Pyne, S.J., 2009. Fire in the Earth system. Science 324 (5926), 481–484.

Callen, M.S., Iturmendi, A., Lopez, J.M., 2014. Source apportionment of atmospheric PM2.5-bound polycyclic aromatic hydrocarbons by a PMF receptor model. Assessment of potential risk for human health. Environ. Pollut. 195, 167–177. https://doi.org/10.1016/j.envpol.2014.08.025.

Carder, K.L., Steward, R.G., Betzer, P.R., Johnson, D.L., Prospero, J.M., 1986. Dynamics and composition of particles from an aeolian input event to the Sargasso Sea. J. Geophys. Res. 91 (D1), 1055. https://doi.org/10.1029/JD091iD01p01055.

Chen, M.R., Tsai, P.J., Wang, Y.F., 2008. Assessing inhalatory and dermal exposures and their resultant health-risks for workers exposed to polycyclic aromatic hydrocarbons (PAHs) contained in oil mists in a fastener manufacturing industry. Environ. Int. 34 (7), 971–975. https://doi.org/10.1016/j.envint.2008.02.008.

Chiu, J.C., Shen, Y.H., Li, H.W., Chang, S.S., Wang, L.C., Chang-Chien, G.P., 2011. Effect of biomass open burning on particulate matter and polycyclic aromatic hydrocarbon concentration levels and PAH dry deposition in ambient air. J. Environ. Sci. Health., Part A 46 (2), 188–197. https://doi.org/10.1080/10934529.2011.532438.

Cogliano, V., Baan, R., Straif, K., Grosse, Y., Secretan, B., Ghissassi, F.E., 2005. Carcinogenicity of human papillomaviruses. Lancet Oncol. 6 (4), 204.

Collins, J.F., Brown, J.P., Alexeeff, G.V., Salmon, A.G., 1998. Potency equivalency factors for some polycyclic aromatic hydrocarbons and polycyclic aromatic hydrocarbon derivatives. Regul. Toxicol. Pharm. 28 (1), 45–54. https://doi.org/10.1006/rtph.1998.1235.

EEA, 2019. Air quality in Europe - 2019 report. Retrieved from https://www.eea.europa.eu/publications/air-quality-in-europe-2019.

EPA, 1993. Provisional guidance for quantitative risk assessment of polycyclic aromatic hydrocarbons. Retrieved from https://nepis.epa.gov/Exe/ZyPURL.cgi?Dockey=30002TUA.txt.

Ezike, C.O., Ohen, J.N., Echor Felix, O., 2017. Assessment of Polycyclic Aromatic Hydrocarbons (Pahs) in Hardwood, Palmwood and Softwood - Smoked Fish. Int. J. Ecotoxicol. Ecobiol. 2 (4) https://doi.org/10.11648/j.ijee.20170204.17.

Feng, B., Li, L., Xu, H., Wang, T., Wu, R., Chen, J., Zhang, Y.i., Liu, S., Ho, S.S.H., Cao, J., Huang, W., 2019. PM2.5-bound polycyclic aromatic hydrocarbons (PAHs) in Beijing: Seasonal variations, sources, and risk assessment. J. Environ. Sci. (China) 77, 11–19. https://doi.org/10.1016/j.jes.2017.12.025.

Friedman, C.L., Selin, N.E., 2012. Long-range atmospheric transport of polycyclic aromatic hydrocarbons: a global 3-D model analysis including evaluation of Arctic sources. Environ. Sci. Technol. 46 (17), 9501–9510. https://doi.org/10.1021/es301904d.

Friedman, C.L., Selin, N.E., 2016. PCBs in the Arctic atmosphere: determining important driving forces using a global atmospheric transport model. Atmos. Chem. Phys. 16 (5), 3433–3448. https://doi.org/10.5194/acp-16-3433-2016.

Friedman, C.L., Zhang, Y., Selin, N.E., 2014. Climate change and emissions impacts on atmospheric PAH transport to the Arctic. Environ. Sci. Technol. 48 (1), 429–437. https://doi.org/10.1021/es403098w.

Giglio, L., Loboda, T., Roy, D.P., Quayle, B., Justice, C.O., 2009. An active-fire based burned area mapping algorithm for the MODIS sensor. Remote Sens. Environ. 113 (2), 408–420. https://doi.org/10.1016/j.rse.2008.10.006.

Giglio, L., Randerson, J.T., van der Werf, G.R., 2013. Analysis of daily, monthly, and annual burned area using the fourth-generation global fire emissions database (GFED4). J. Geophys. Res. Biogeosci. 118 (1), 317–328. https://doi.org/10.1002/jgrg.20042.

Hassan, S.K., Khoder, M.I., 2012. Gas-particle concentration, distribution, and health risk assessment of polycyclic aromatic hydrocarbons at a traffic area of Giza. Egypt. *Environ Monit Assess* 184 (6), 3593–3612. https://doi.org/10.1007/s10661-011-2210-8.

Hoseini, M., Yunesian, M., Nabizadeh, R., Yaghmaeian, K., Ahmadkhaniha, R., Rastkari, N., Parmy, S., Faridi, S., Rafiee, A., Naddafi, K., 2016. Characterization and risk assessment of polycyclic aromatic hydrocarbons (PAHs) in urban atmospheric Particulate of Tehran, Iran. Environ. Sci. Pollut. Res. Int. 23 (2), 1820–1832. https://doi.org/10.1007/s11356-015-5355-0.

Huang, T., Ling, Z., Ma, J., Macdonald, R.W., Gao, H., Tao, S., Tian, C., Song, S., Jiang, W., Chen, L., Chen, K., Xie, Z., Zhao, Y., Zhao, L., Gu, C., Mao, X., 2020. Human exposure to polychlorinated biphenyls embodied in global fish trade. Nature Food 1 (5), 292–300. https://doi.org/10.1038/s43016-020-0066-1.

IARC, 2021. Agents classified by the IARC monographs, vol. 1–129. Retrieved from http://monographs.iarc.fr/ENG/Classification/index.

IPCC, 2014. Climate Change 2014: Synthesis Report. In: Pachauri, R.K., Meyer, L. (Eds.), Contribution of Working Groups I, II and III to the Fifth Assessment Report of the Intergovernmental Panel on Climate Change. Geneva, Switzerland.

Jolly, W.M., Cochrane, M.A., Freeborn, P.H., Holden, Z.A., Brown, T.J., Williamson, G.J., Bowman, D.M., 2015. Climate-induced variations in global wildfire danger from 1979 to 2013. Nat. Commun. 6, 7537. https://doi.org/10.1038/ncomms8537.

Kaiser, J.W., Heil, A., Andreae, M.O., Benedetti, A., Chubarova, N., Jones, L., Morcrette, J.-J., Razinger, M., Schultz, M.G., Suttie, M., van der Werf, G.R., 2012. Biomass burning emissions estimated with a global fire assimilation system based on observed fire radiative power. Biogeosciences 9 (1), 527–554. https://doi.org/10.5194/bg-9-527-2012.

Kalisa, E., Nagato, E.G., Bizuru, E., Lee, K.C., Tang, N., Pointing, S.B., Hayakawa, K., Archer, S.D.J., Lacap-Bugler, D.C., 2018. Characterization and Risk Assessment of Atmospheric PM2.5 and PM10 Particulate-Bound PAHs and NPAHs in Rwanda, Central-East Africa. Environ. Sci. Technol. 52 (21), 12179–12187. https://doi.org/10.1021/acs.est.8b0321910.1021/acs.est.8b03219.s001.

Ke, C.L., Gu, Y.G., Liu, Q., Li, L.D., Huang, H.H., Cai, N., Sun, Z.W., 2017. Polycyclic aromatic hydrocarbons (PAHs) in wild marine organisms from South China Sea: Occurrence, sources, and human health implications. Mar. Pollut. Bull. 117 (1–2), 507–511. https://doi.org/10.1016/j.marpolbul.2017.02.018.

Kim, K.H., Jahan, S.A., Kabir, E., Brown, R.J., 2013. A review of airborne polycyclic aromatic hydrocarbons (PAHs) and their human health effects. Environ. Int. 60, 71–80. https://doi.org/10.1016/j.envint.2013.07.019.

Lammel, G., Heil, A., Stemmler, I., Dvorska, A., Klanova, J., 2013. On the contribution of biomass burning to POPs (PAHs and PCDDs) in air in Africa. Environ. Sci. Technol. 47 (20), 11616–11624. https://doi.org/10.1021/es401499q.

Langmann, B., Duncan, B., Textor, C., Trentmann, J., van der Werf, G.R., 2009. Vegetation fire emissions and their impact on air pollution and climate. Atmos. Environ. 43 (1), 107–116. https://doi.org/10.1016/j.atmosenv.2008.09.047.

Le Bihanic, F., Clerandeau, C., Le Menach, K., Morin, B., Budzinski, H., Cousin, X., Cachot, J., 2014. Developmental toxicity of PAH mixtures in fish early life stages. Part II: adverse effects in Japanese medaka. Environ. Sci. Pollut. Res. Int. 21 (24), 13732–13743. https://doi.org/10.1007/s11356-014-2676-3.

Lian, L., Huang, T., Ling, Z., Li, S.i., Li, J., Jiang, W., Gao, H., Tao, S., Liu, J., Xie, Z., Mao, X., Ma, J., 2021. Interprovincial trade driven relocation of polycyclic aromatic hydrocarbons and lung cancer risk in China. J. Cleaner Prod. 280, 124368. https://doi.org/10.1016/j.jclepro.2020.124368.

Lian, L., Huang, T., Ke, X., Ling, Z., Jiang, W., Wang, Z., Song, S., Li, J., Zhao, Y., Gao, H., Tao, S., Liu, J., Ma, J., 2022. Globalization-Driven Industry Relocation Significantly Reduces Arctic PAH. Environ. Sci. Technol. 56, 145–154. https://doi.org/10.1021/acs.est.1c05198.

Liousse, C., Assamoi, E., Criqui, P., Granier, C., Rosset, R., 2014. Explosive growth in African combustion emissions. Environ. Res. Lett. 9 (3), 035003. https://doi.org/10.1088/1748-9326/9/3/035003.

Luo, J., Han, Y., Zhao, Y., Huang, Y., Liu, X., Tao, S., Liu, J., Huang, T., Wang, L., Chen, K., Ma, J., 2020. Effect of northern boreal forest fires on PAH fluctuations across the arctic. Environ. Pollut. 261, 114186. https://doi.org/10.1016/j.envpol.2020.114186.

Ma, J., Daggupaty, S., Harner, T., Li, Y., 2003. Impacts of lindane usage in the Canadian prairies on the Great Lakes ecosystem. 1. Coupled atmospheric transport model and

modeled concentrations in air and soil. Environ. Sci. Technol. 37 (17), 3774–3781. https://doi.org/10.1021/es034160x.
MacLeod, M., Fraser, A.J., Mackay, D., 2002. Evaluating and expressing the propagation of uncertainty in chemical fate and bioaccumulation models. Environ. Toxicol. Chem. 21 (4), 700–709. https://doi.org/10.1002/etc.5620210403.
Mattsson, J.O., Nihlén, T., 1996. The transport of Saharan dust to southern Europe: a scenario. J. Arid Environ. 32 (2), 111–119. https://doi.org/10.1006/jare.1996.0011.
Menzie, C.A., Potocki, B.B., Santodonato, J., 2002. Exposure to carcinogenic PAHs in the environment. Environ. Sci. Technol. 26 (7), 1278–1284. https://doi.org/10.1021/es00031a002.
Ofori, S.A., Cobbina, S.J., Doke, D.A., 2020. The occurrence and levels of polycyclic aromatic hydrocarbons (PAHs) in African environments-a systematic review. Environ. Sci. Pollut. Res. Int. 27 (26), 32389–32431. https://doi.org/10.1007/s11356-020-09428-2.
Orakij, W., Chetiyanukornkul, T., Kasahara, C., Boongla, Y., Chuesaard, T., Furuuchi, M., Hata, M., Tang, N., Hayakawa, K., Toriba, A., 2017. Polycyclic aromatic hydrocarbons and their nitro derivatives from indoor biomass-fueled cooking in two rural areas of Thailand: a case study. Air Qual. Atmos. Health 10 (6), 747–761. https://doi.org/10.1007/s11869-017-0467-y.
Pan, Y., Birdsey, R.A., Fang, J., Houghton, R., Kauppi, P.E., Kurz, W.A., Phillips, O.L., Shvidenko, A., Lewis, S.L., Canadell, J.G., Ciais, P., Jackson, R.B., Pacala, S.W., McGuire, A.D., Piao, S., Rautiainen, A., Sitch, S., Hayes, D., 2011. A large and persistent carbon sink in the world's forests. Science 333 (6045), 988–993.
Perry, K.D., Cahill, T.A., Eldred, R.A., Dutcher, D.D., Gill, T.E., 1997. Long-range transport of North African dust to the eastern United States. J. Geophys. Res. Atmosph. 102 (D10), 11225–11238. https://doi.org/10.1029/97jd00260.
Prodi, F., Fea, G., 1979. A case of transport and deposition of Saharan dust over the Italian Peninsula and southern Europe. J. Geophys. Res. 84 (C11), 6951. https://doi.org/10.1029/JC084iC11p06951.
Prospero, J.M., Carlson, T.N., 1972. Vertical and areal distribution of Saharan dust over the western equatorial north Atlantic Ocean. J. Geophys. Res. 77 (27), 5255–5265. https://doi.org/10.1029/JC077i027p05255.
Prospero, J.M., Glaccum, R.A., Nees, R.T., 1981. Atmospheric transport of soil dust from Africa to South America. Nature 289 (5798), 570–572. https://doi.org/10.1038/289570a0.
Ramirez, N., Cuadras, A., Rovira, E., Marce, R.M., Borrull, F., 2011. Risk assessment related to atmospheric polycyclic aromatic hydrocarbons in gas and particle phases near industrial sites. Environ. Health Perspect. 119 (8), 1110–1116. https://doi.org/10.1289/ehp.1002855.
Ravindra, K., Sokhi, R., Vangrieken, R., 2008. Atmospheric polycyclic aromatic hydrocarbons: Source attribution, emission factors and regulation. Atmos. Environ. 42 (13), 2895–2921. https://doi.org/10.1016/j.atmosenv.2007.12.010.
Rengarajan, T., Rajendran, P., Nandakumar, N., Lokeshkumar, B., Rajendran, P., Nishigaki, I., 2015. Exposure to polycyclic aromatic hydrocarbons with special focus on cancer. Asian Pacif. J. Trop. Biomed. 5 (3), 182–189. https://doi.org/10.1016/s2221-1691(15)30003-4.
Rossner Jr., P., Topinka, J., Hovorka, J., Milcova, A., Schmuczerova, J., Krouzek, J., Sram, R.J., 2010. An acellular assay to assess the genotoxicity of complex mixtures of organic pollutants bound on size segregated aerosol. Part II: oxidative damage to DNA. Toxicol. Lett. 198 (3), 312–316. https://doi.org/10.1016/j.toxlet.2010.06.021.
Sarigiannis, D., Karakitsios, S.P., Zikopoulos, D., Nikolaki, S., Kermenidou, M., 2015. Lung cancer risk from PAHs emitted from biomass combustion. Environ. Res. 137, 147–156. https://doi.org/10.1016/j.envres.2014.12.009.
Savoie, D.L., Prospero, J.M., 1977. Aerosol concentration statistics for the Northern Tropical Atlantic. J. Geophys. Res. 82 (37), 5954–5964. https://doi.org/10.1029/JC082i037p05954.
Sexton, K., Linder, S.H., Marko, D., Bethel, H., Lupo, P.J., 2007. Comparative assessment of air pollution-related health risks in Houston. Environ. Health Perspect. 115 (10), 1388–1393. https://doi.org/10.1289/ehp.10043.
Shen, H., Huang, Y.e., Wang, R., Zhu, D., Li, W., Shen, G., Wang, B., Zhang, Y., Chen, Y., Lu, Y., Chen, H., Li, T., Sun, K., Li, B., Liu, W., Liu, J., Tao, S., 2013. Global atmospheric emissions of polycyclic aromatic hydrocarbons from 1960 to 2008 and future predictions. Environ. Sci. Technol. 47 (12), 6415–6424. https://doi.org/10.1021/es400857z.
Shen, H., Tao, S., Liu, J., Huang, Y.e., Chen, H., Li, W., Zhang, Y., Chen, Y., Su, S., Lin, N., Xu, Y., Li, B., Wang, X., Liu, W., 2014. Global lung cancer risk from PAH exposure highly depends on emission sources and individual susceptibility. Sci. Rep. 4 (1) https://doi.org/10.1038/srep06561.
Situma, D.S., 2010. Assessment of polycyclic aromatic hydrocarbons (PAHs) in air and soil from selected sites in Nairobi, (Master),. University of Nairobi.
Sram, R.J., Beskid, O., Rössnerova, A., Rössner, P., Lnenickova, Z., Milcova, A., Solansky, I., Binkova, B., 2007. Environmental exposure to carcinogenic polycyclic aromatic hydrocarbons–the interpretation of cytogenetic analysis by FISH. Toxicol. Lett. 172 (1-2), 12–20. https://doi.org/10.1016/j.toxlet.2007.05.019.
Stuut, J.B., Smalley, I., O'Hara-Dhand, K., 2009. Aeolian dust in Europe: African sources and European deposits. Quat. Int. 198 (1–2), 234–245. https://doi.org/10.1016/j.quaint.2008.10.007.
Tsai, P.-J., Shieh, H.-Y., Lee, W.-J., Lai, S.-O., 2001. Health-risk assessment for workers exposed to polycyclic aromatic hydrocarbons (PAHs) in a carbon black manufacturing industry. Sci. Total Environ. 278 (1–3), 137–150. https://doi.org/10.1016/s0048-9697(01)00643-x.
van der Werf, G.R., Randerson, J.T., Giglio, L., Collatz, G.J., Mu, M., Kasibhatla, P.S., Morton, D.C., DeFries, R.S., Jin, Y., van Leeuwen, T.T., 2010. Global fire emissions and the contribution of deforestation, savanna, forest, agricultural, and peat fires (1997–2009). Atmos. Chem. Phys. 10 (23), 11707–11735. https://doi.org/10.5194/acp-10-11707-201010.5194/acp-10-11707-2010-supplement.
Verma, P.K., Sah, D., Kumari, K.M., Lakhani, A., 2017. Atmospheric concentrations and gas-particle partitioning of polycyclic aromatic hydrocarbons (PAHs) and nitro-PAHs at Indo-Gangetic sites. Environ. Sci. Process. Impacts 19 (8), 1051–1060. https://doi.org/10.1039/c7em00168a.
Wang, R., Liu, G., Zhang, J., 2015. Variations of emission characterization of PAHs emitted from different utility boilers of coal-fired power plants and risk assessment related to atmospheric PAHs. Sci. Total Environ. 538, 180–190. https://doi.org/10.1016/j.scitotenv.2015.08.043.
WHO, 2017. Evolution of WHO air quality guidelines: past, present and future. Copenhagen: WHO Regional Office for Europe. WHO Regional Office for Europe UN City, Copenhagen, Denmark.
Wilcke, W., 2007. Global patterns of polycyclic aromatic hydrocarbons (PAHs) in soil. Geoderma 141 (3–4), 157–166. https://doi.org/10.1016/j.geoderma.2007.07.007.
Yu, Y., Katsoyiannis, A., Bohlin-Nizzetto, P., Brorström-Lundén, E., Ma, J., Zhao, Y., Wu, Z., Tych, W., Mindham, D., Sverko, E.d., Barresi, E., Dryfhout-Clark, H., Fellin, P., Hung, H., 2019. Polycyclic Aromatic Hydrocarbons Not Declining in Arctic Air Despite Global Emission Reduction. Environ. Sci. Technol. 53 (5), 2375–2382. https://doi.org/10.1021/acs.est.8b0535310.1021/acs.est.8b05353.s001.
Zedeck, M.S., 1980. Polycyclic aromatic hydrocarbons: A review. J. Environ. Pathol. Toxicol. 3, 537–567.
Zhang, L., Ma, J., Venkatesh, S., Li, Y.F., Cheung, P., 2008. Modeling evidence of episodic intercontinental long-range transport of lindane. Environ. Sci. Technol. 42 (23), 8791–8797. https://doi.org/10.1021/es801271b.
Zhang, Y., Chen, X., Zhang, Y.u., 2021. Analytical chemistry, formation, mitigation, and risk assessment of polycyclic aromatic hydrocarbons: From food processing to in vivo metabolic transformation. Compr. Rev. Food Sci. Food Saf. 20 (2), 1422–1456. https://doi.org/10.1111/1541-4337.12705.
Zhang, Y., Tao, S., 2009. Global atmospheric emission inventory of polycyclic aromatic hydrocarbons (PAHs) for 2004. Atmos. Environ. 43 (4), 812–819. https://doi.org/10.1016/j.atmosenv.2008.10.050.
Zheng, H., Xing, X., Hu, T., Zhang, Y., Zhang, J., Zhu, G., Li, Y., Qi, S., 2018. Biomass burning contributed most to the human cancer risk exposed to the soil-bound PAHs from Chengdu Economic Region, western China. Ecotoxicol. Environ. Saf. 159, 63–70. https://doi.org/10.1016/j.ecoenv.2018.04.065.

Further reading

Bari, M.A., Baumbach, G., Kuch, B., Scheffknecht, G., 2011. Air Pollution in Residential Areas from Wood-fired Heating. Aerosol Air Qual. Res. 11 (6), 749–757. https://doi.org/10.4209/aaqr.2010.09.0079.
Hattemer-Frey, H.A., Travis, C.C., 1991. Benzo-a-pyrene: environmental partitioning and human exposure. Toxicol. Ind. Health 7 (3), 141–157. https://doi.org/10.1177/074823379100700303.
Jiang, W., Chen, H., Huang, T., Lian, L., Li, J., Jia, C., Gao, H., Mao, X., Ma, J., 2019. Tagged sources of short-chain chlorinated paraffins in China's marine environment and fish. Chemosphere 229, 358–365. https://doi.org/10.1016/j.chemosphere.2019.04.144.
Kim, E.-J., Oh, J.-E., Chang, Y.-S., 2003. Effects of forest fire on the level and distribution of PCDD/Fs and PAHs in soil. Sci. Total Environ. 311 (1–3), 177–189. https://doi.org/10.1016/s0048-9697(03)00095-0.
Laflamme, R.E., Hites, R.A., 1978. The global distribution of polycyclic aromatic hydrocarbons in recent sediments. Geochim. Cosmochim. Acta 42 (3), 289–303. https://doi.org/10.1016/0016-7037(78)90182-5.
Perera, F.P., 1997. Environment and cancer: who are susceptible? Science 278 (5340), 1068–1073. https://doi.org/10.1126/science.278.5340.1068.
Pradhan, A., Carvalho, F., Abrantes, N., Campos, I., Keizer, J.J., Cássio, F., Pascoal, C., 2020. Biochemical and functional responses of stream invertebrate shredders to post-wildfire contamination. Environ. Pollut. 267, 115433. https://doi.org/10.1016/j.envpol.2020.115433.
Toyooka, T., Ibuki, Y., 2007. DNA damage induced by coexposure to PAHs and light. Environ. Toxicol. Pharmacol. 23 (2), 256–263. https://doi.org/10.1016/j.etap.2006.09.002.
Tsiodra, I., Grivas, G., Tavernaraki, K., Bougiatioti, A., Apostolaki, M., Paraskevopoulou, D., Mihalopoulos, N., 2021. Annual exposure to PAHs in urban environments linked to wintertime wood-burning episodes. Atmosph. Chem. Phys. Discuss. https://doi.org/10.5194/acp-2021-393.
Wang, J., Chen, S., Tian, M.i., Zheng, X., Gonzales, L., Ohura, T., Mai, B., Simonich, S.L. M., 2012. Inhalation cancer risk associated with exposure to complex polycyclic aromatic hydrocarbon mixtures in an electronic waste and urban area in South China. Environ. Sci. Technol. 46 (17), 9745–9752. https://doi.org/10.1021/es302272a.
Wild, S.R., Jones, K.C., 1995. Polynuclear aromatic hydrocarbons in the United Kingdom environment: A preliminary source inventory and budget. Environ. Pollut. 88 (1), 91–108. https://doi.org/10.1016/0269-7491(95)91052-m.
Yoon, E., Park, K., Lee, H., Yang, J.-H., Lee, C., 2007. Estimation of Excess Cancer Risk on Time-Weighted Lifetime Average Daily Intake of PAHs from Food Ingestion. Human Ecol. Risk Assess. Int. J. 13 (3), 669–680. https://doi.org/10.1080/10807030701226871.
Zhang, L., Ma, J., Tian, C., Li, Y., Hung, H., 2010. Atmospheric transport of persistent semi-volatile organic chemicals to the Arctic and cold condensation in the mid-troposphere – Part 2: 3-D modeling of episodic atmospheric transport. Atmos. Chem. Phys. 10 (15), 7315–7324. https://doi.org/10.5194/acp-10-7315-2010.